Specificity of Cone Inputs to Macaque Retinal Ganglion Cells

Hao Sun, Hannah E. Smithson, Qasim Zaidi and Barry B. Lee

You might find this additional info useful...

A corrigendum for this article has been published. It can be found at:
http://jn.physiology.org/content/104/1/578.full.html

This article cites 51 articles, 14 of which can be accessed free at:
http://jn.physiology.org/content/95/2/837.full.html#ref-list-1

This article has been cited by 12 other HighWire hosted articles, the first 5 are:

Latency characteristics of the short-wavelength-sensitive cones and their associated pathways
R. J. Lee, J. D. Mollon, Q. Zaidi and H. E. Smithson
J Vis, November, 12 2009; 9 (12): .
[Abstract] [Full Text] [PDF]

Temporal structure of chromatic channels revealed through masking
John Cass, Colin W. G. Clifford, David Alais and Branka Spehar
J Vis, May, 18 2009; 9 (5): .
[Abstract] [Full Text] [PDF]

The S-cone contribution to luminance depends on the M- and L-cone adaptation levels: Silent surrounds?
Caterina Ripamonti, Wen Ling Woo, Elizabeth Crowther and Andrew Stockman
J Vis, March, 13 2009; 9 (3): .
[Abstract] [Full Text] [PDF]

Updated information and services including high resolution figures, can be found at:
http://jn.physiology.org/content/95/2/837.full.html

Additional material and information about *Journal of Neurophysiology* can be found at:
http://www.the-aps.org/publications/jn

This infomation is current as of December 21, 2010.

Specificity of Cone Inputs to Macaque Retinal Ganglion Cells

Hao Sun,[1] Hannah E. Smithson,[2] Qasim Zaidi,[1] and Barry B. Lee[1,3]

[1]*State University of New York, State College of Optometry, New York, New York;* [2]*Department of Psychology,*
Durham University, Durham, United Kingdom; and [3]*Max Planck Institute for Biophysical Chemistry, Göttingen, Germany*

Sun, Hao, Hannah E. Smithson, Qasim Zaidi, and Barry B. Lee.
Specificity of cone inputs to macaque retinal ganglion cells. *J Neu-rophysiol* 95: 837–849, 2006; doi:10.1152/jn.00714.2005. The spec-ificity of cone inputs to ganglion cells has implications for the development of retinal connections and the nature of information transmitted to higher areas of the brain. We introduce a rapid and precise method for measuring signs and magnitudes of cone inputs to visual neurons. Colors of stimuli are modulated around circumfer-ences of three color planes in clockwise and counterclockwise direc-tions. For each neuron, the projection of the preferred vector in each plane was estimated by averaging the response phases to clockwise and counterclockwise modulation. The signs and weights of cone inputs were derived directly from the preferred vectors. The efficiency of the method enables us to measure cone inputs at different temporal frequencies and short-wavelength-sensitive (S) cone adaptation levels. The results show that S-cone inputs to the parvocellular and magno-cellular ganglion cells are negligible, which implies underlying con-nectional specificity in the retinal circuitry.

INTRODUCTION

Visual processing in primates starts with light absorption in three classes of cones [short- (S), middle- (M), and long-wavelength (L) sensitive]. When lights are represented in a three-dimensional (3-D) cone space, L- and M-cone dimen-sions are highly correlated because of their overlapping ab-sorption spectra (Smith and Pokorny 1972). Postreceptoral neurons in the retina add and subtract cone outputs to reduce redundancy in the information transmitted to cortex (Buchs-baum and Gottschalk 1983; Zaidi 1997). Knowledge of cone inputs to postreceptoral neurons is fundamental for understand-ing retinal circuitry and the nature of visual information pro-cessing.

A classical method of measuring cone inputs to visual neurons was introduced by Derrington et al. (1984). They used stimuli modulated through white in various orientations in a 3-D color space, defined by an L+M+S axis, a constant S-cone axis, and a constant L- and M-cone axis (DKL space). For each linear visual neuron, there exists a single null plane through white that contains all the lights that can be exchanged without inducing a response. Derrington et al. inferred cone inputs from cells' null planes.

If a cell receives only M- and L-cone inputs, its null plane should pass through the constant L- and M-cone axis. Der-rington et al. found that the null planes of lateral geniculate nucleus (LGN) neurons in both parvocellular (PC) and mag-nocellular (MC) layers showed some scatter around this axis. This could be caused by measurement uncertainty or actual

S-cone input. S-cone input to MC cells is relevant to whether this pathway is the physiological substrate of a psychophysical luminance channel (Kaiser et al. 1990; Lee et al. 1988). For a psychophysical luminance channel, it is generally accepted that there is little S-cone input (Lennie et al. 1993), although under extreme adaptation conditions some contribution of S cones to flicker nulls may be present (Stockman et al. 1991, 1993). On photometric tasks, the MC pathway seems to be the substrate of a psychophysical luminance channel (Lee et al. 1988) and has a spectral sensitivity similar to the luminosity function. However, recently, Chatterjee and Callaway (2002) measured responses of LGN neurons to luminance and S-cone modula-tion and claimed that there is about 7% S-cone input to LGN cells of the MC layers. We will argue that this result was caused by the use of inappropriate estimates of cone funda-mentals.

The cone input to ganglion cells has implications for the specificity of retinal wiring. Although PC cells' surrounds could draw inputs from mixed cone types (Lennie et al. 1991; Mullen and Kingdom 1996), experimental evidence suggests surrounds may be cone specific (Lee et al. 1998; Reid and Shapley 1992, 2002). Whether cells receive random or cone-specific input touches on a central issue in retinal circuitry, and the presence or absence of S-cone inputs to PC or MC cells is a test of wiring specificity.

We present a novel method to measure cone inputs to visual neurons. We modulated the color of a uniform field clockwise (CW) or counterclockwise (CCW) around the circumference of a circle in each of three color planes and measured ganglion cells' response phases. Cone weights were estimated from the preferred vector, calculated as the average of CW and CCW response phases, which cancels out phase lags. One advantage of this method is that it is a measurement of response phase, which is a stable feature of cell behavior. The method is rapid and precise, and its efficiency permits exploration of different frequencies and adaptation conditions. We used the technique to investigate L-, M-, and S-cone inputs. Our data show that most of the scatter of PC and MC ganglion cells' preferred vectors is caused by factors other than actual S-cone input.

METHODS

Rationale

The stimulus was first introduced by Zaidi and Halevy (1991) and used in psychophysical experiments by Stromeyer et al. (1991) and Zaidi and Halevy (1993). The chromaticity of a uniform field is modulated around the circumference of a color circle in a CW or

---

Address for reprint requests and other correspondence: H. Sun, State Univ. of New York, State College of Optometry, 33 West 42nd St., New York, NY 10036 (E-mail: hsun@sunyopt.edu).

CCW direction (Fig. 1). An advantage of using such stimuli is that the modulation of each cone type is a sinusoidal function, and so is the modulation of any linear combination of cone signals, such as an L-M opponent signal or an L+M luminance signal. In Fig. 1, *A1, B1,* and *C1* show the stimulus modulation in the equiluminant plane, the L- versus M-cone plane and the L+M versus S-cone plane, and the Boynton-Kambe (Boynton and Kambe 1980) chromaticity coordinates (l, m, s) at selected color angles. Figure 1, *A2, B2,* and *C2,* shows the modulation of L-, M-, and S-cone signals as a function of color angle in each plane, and Fig. 1, *A3, B3,* and *C3,* shows the modulation of L-M, L+M, and S-(L+M) signals.

For a neuron that receives cone inputs $w_lL + w_mM + w_sS$, the preferred vector is defined by cone weights (w_l,w_m,w_s). The preferred vector determines the phase of the combined cone signals, and modulation along it produces the maximal response. For example, a neuron that receives only L-M input has a preferred vector that projects to 0° in the equiluminant plane, and a neuron that receives S-(L+M) input has a preferred vector that projects to 90° in the equiluminant plane. If a cell receives L-M input plus some S-cone signal, an intermediate preferred vector between 0 and 90° will result.
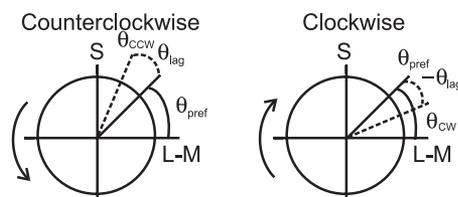

FIG. 2.   For a linear neuron, the preferred vector θ_{pref} does not change from CW to CCW modulation, whereas the phase delay θ_{lag} changes its sign from CW to CCW modulation. Averaging CW and CCW response phases cancels θ_{lag} to reveal the cell's preferred vector θ_{pref} in the stimulus plane.

We define each cycle of modulation as a complete 360° excursion around the circumference of a circle in the plane. Hence each phase of the temporal modulation has a one-to-one relationship to color angle. When a cell's response histogram is plotted versus the stimulus angle and fitted with Fourier harmonics, the stimulus angle at the peak of the first harmonic is called the cell's response phase.

A cell's response phase to CCW modulation, θ_{CCW}, or to CW modulation, θ_{CW}, equals the sum of the cell's preferred vector θ_{pref} and an intrinsic phase delay θ_{lag} (Fig. 2). The preferred vector θ_{pref} of
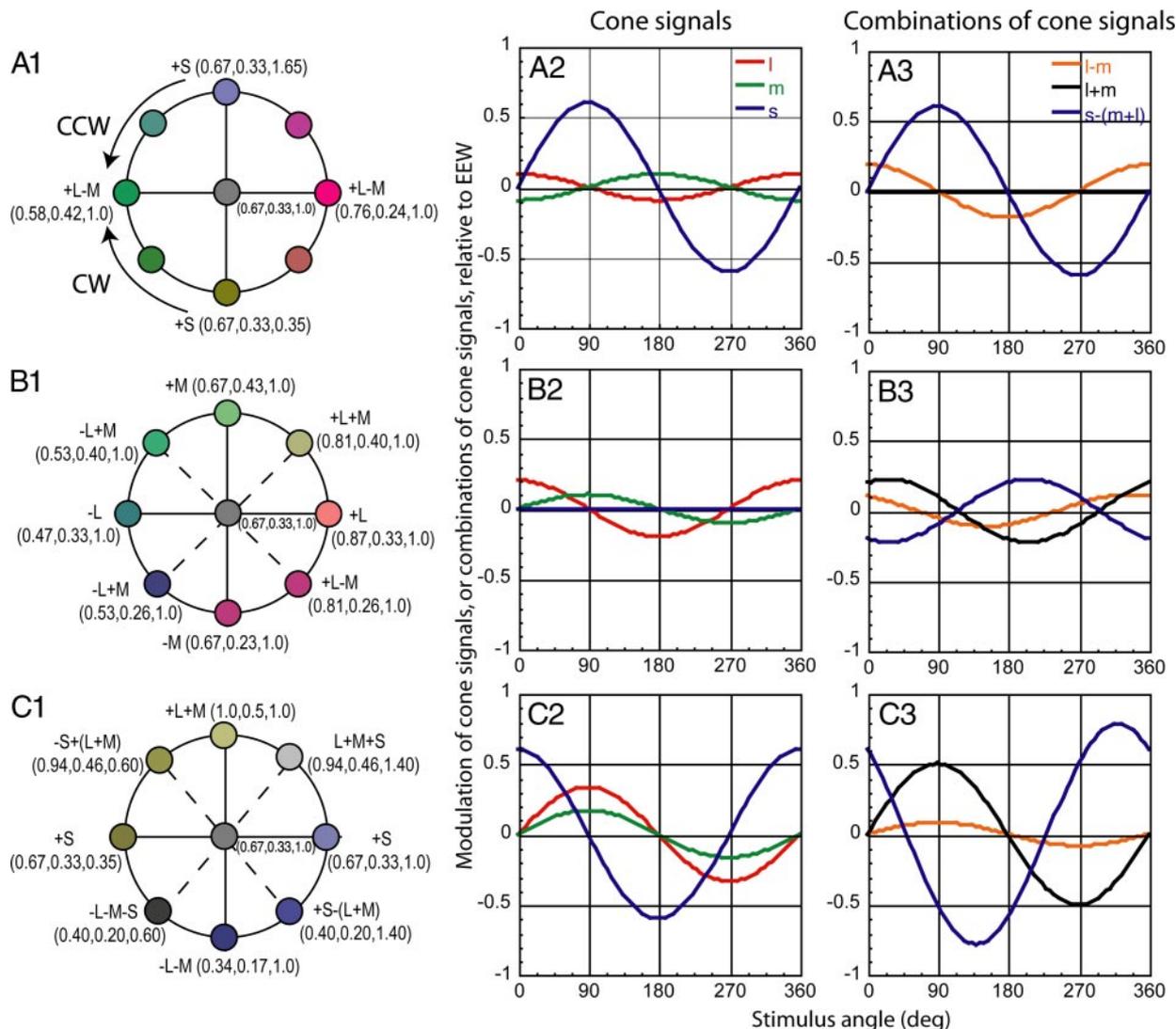

FIG. 1.   Chromaticity of a uniform field was modulated around a color circle in clockwise (CW) or counterclockwise (CCW) directions in an equiluminant plane (*A1*), an long (L)- vs. medium (M)-cone plane (*B1*), or an L+M vs. short (S)-cone plane (*C1*). Numbers in *A1–C1* indicate Boynton-Kambe chromaticity coordinates (L, M, S) for each point, and colored circles approximate stimulus appearance. Variation of L-, M-, and S-cone signals for the 3 planes are shown in *A2–C2,* and combinations of cone signals L-M, L+M, and S-(L+M) are shown in *A3–C3,* respectively. *C1–C3*: 50% L+M contrast condition.

a neuron is determined by the cell's cone inputs, and it does not change from CW to CCW modulation; but the phase delay θ_{lag}, which is caused by latency and other factors, changes its sign from CW to CCW modulation. Averaging θ_{CCW} and θ_{CW} will cancel the phase delay term θ_{lag} to give the cell's preferred vector θ_{pref} in that stimulus plane (see APPENDIX for details). The preferred vector is orthogonal to the null plane used by Derrington et al. and provides both signs and weights of cone inputs.

Apparatus and calibration

Stimuli were generated by a Maxwellian view system with center and surround fields consisting of four light emitting diodes (LEDs) and matched interference filters (Pokorny et al. 2004). Only three of the four LEDs from one field were used in the experiment. The system was controlled by a Macintosh Quadra 950 computer. For calibration, we first measured the spectral distribution of each LED and interference filter combination at 2-nm intervals at the pupil locus using a spectroradiometer (Spectrascan 704, Photo Research, Chatsworth, CA). The peak wavelengths of the LED interference filter combinations were 460, 518, and 660 nm, and half-height bandwidths were 8–10 nm. We calculated the chromaticity and relative luminance of each spectral channel by multiplying each spectrum with cone fundamentals that were obtained by applying the Smith-Pokorny transformation (Smith and Pokorny 1975) to the CIE 1964 10° color matching functions and the 10° V_λ luminosity function (Shapiro et al. 1996). The cone excitations were normalized so that the L-, M-, and S-cone excitations of 1 unit of light metameric to the equal energy spectrum white (EEW) are (0.667, 0.333, 1) (Boynton and Kambe 1980). Human cone fundamentals provide good estimates of the macaque cone spectra given the similarity in cone spectra (Baylor et al. 1987), prereceptoral filters (lens and macular pigment), and optical density (Snodderly et al. 1984). Last, we measured the maximum photopic illuminance of the 660-nm channel with a photometer (Spectraspotmeter, Photo Research Division Kollmorgen, Burbank, CA) (Westheimer 1966) and used this as a standard to calculate the absolute illuminance of the other two channels.

Stimulus

The stimulus was a 4.7° (diam) spatially uniform field. The chromaticity of the stimulus was modulated around the circumference of a color circle in a CCW or CW direction in three color planes (Fig. 1). The mean chromaticity of the modulation, i.e., the center of the color circle in each plane, was metameric to EEW. The mean illuminance was 2398 td. The axes of the planes are defined as follows. In the equiluminant plane, along the L-M axis, L- to M-cone excitations exchange so that the luminance (L+M, with L- and M-cone excitation ratio of 2:1) and S-cone excitation are constant; along the S-cone axis, S-cone excitation changes, whereas L- and M-cone excitations are kept constant. In the L- versus M-cone plane, along the L-cone axis, L-cone excitation changes, whereas M- and S-cone excitations are kept constant, and along the M-cone axis, M-cone excitation changes, whereas L- and S-cone excitations are kept constant. In the L+M versus S-cone plane, along the S-cone axis, S-cone excitation changes, whereas L- and M-cone excitations are constant; along the L+M axis, the luminance is modulated, whereas S-cone excitation and the ratio of L- to M-cone excitations are kept constant. Vectors in the first and third quadrants represent additive inputs from the two axes, whereas those in the second and fourth quadrants represent opponent inputs from the two axes. For example, in the L- versus M-cone plane, a vector of 26.6° represents a luminance signal, whereas a vector of 135° represents a L+M signal; in the L+M versus S-cone plane, a vector of 315° represents a +S-(L+M) signal, whereas a vector of 45° represents an L+M+S signal.

Six temporal frequencies were used (1.22, 2.44, 4.88, 9.76, 19.52, and 39.04 Hz). In the equiluminant plane, we used the maximum attainable L-M modulation (14% L-cone contrast and 28% M-cone contrast) to evoke vigorous responses from PC cells. In the L+M versus S-cone plane, we used 50% luminance contrast for PC cells and MC cells at low frequencies (1.22 to 4.88 Hz) and reduced the luminance contrast to 25% for MC cells at high frequencies (9.76 to 39.04 Hz) to minimize phase shifts caused by MC cells' contrast gain controls. We used 65% S-cone contrast for all conditions to help reveal any possible S-cone input. We used 30% L-cone and M-cone contrasts for the L- versus M-cone plane.

In a control experiment designed to distinguish between S-cone inputs and variation in prereceptoral filtering, we repeated measurements in the equiluminant and the L+M versus S-cone planes with the mean chromaticity displaced along an estimated tritanopic confusion line (along which only S-cone excitation is modulated, whereas L- and M-cone excitations are constant) to deliver 1918, 4316, 5755, and 7674 S-cone td (Shapiro et al. 1996).

To compare our technique with that of Derrington et al., we also measured ganglion cell's responses to a stimulus that was modulated along lines of various orientations through the EEW point (Derrington et al. 1984). For each plane, the modulation orientation was varied between 0 and 180°, with a step size of 22.5°. The temporal frequency was either 3.26 or 19.52 Hz.

Procedure

We recorded from the retinae of five anesthetized macaque monkeys (*Macaca fascicularis*). All procedures strictly conformed to the National Institutes of Health Guide for the Care and Use of Laboratory Animals and were approved by the SUNY State College of Optometry Animal Care and Use Committee. The animals were initially sedated with an intramuscular injection of ketamine (10 mg/kg). Anesthesia was induced with sodium thiopental (10 mg/kg) and maintained with inhaled isoflurane (0.2–2%) in a 70:30 N_2O-O_2 mixture. Local anesthetic was applied to points of surgical intervention. EEG and ECG were monitored continuously to ensure animal health and adequate depth of anesthesia. Muscle relaxation was maintained by an infusion of gallamine triethiodide (5 mg/kg/h, iv) with accompanying dextrose Ringer solution (5 ml/kg/h). Body temperature was kept close to 37.5°C. End-tidal CO_2 was kept close to 4% by adjusting the rate and depth of respiration.

Neuronal activity was recorded directly from retinal ganglion cells by an electrode inserted through a cannula entering the eye behind the limbus. A gas-permeable contact lens of the appropriate power was used to bring stimuli into focus on the retina. We recorded responses of cells between 4 and 8° eccentricity. Cell identification was achieved through standard tests (Lee et al. 1989). These included achromatic contrast sensitivity and responses to lights of different chromaticity. Additional tests, e.g., measuring responses to heterochromatically modulated lights (Smith et al. 1992), were used in cases when identification was difficult. PC cells can generally be identified by their tonic responses and spectral opponency and MC cells by their phasic responses and lack of spectral opponency. For each cell, the locus of the receptive field center was determined, and the stimulus was centered on this point. Before collecting data, 8-s adaptation to the mean chromaticity was permitted. Cell responses were recorded to modulation of the spatially uniform stimulus at different temporal frequencies and in the different color planes. Times of spike occurrence were recorded to an accuracy of 0.1 ms, and averaged histograms of spike trains were simultaneously accumulated with 64 bins per cycle of modulation. Numbers of repetitions varied from 8 to 256 cycles depending on the temporal frequency.

Data analysis and estimation of preferred vectors

We performed Fourier analysis on the cells' response histograms and calculated response phases and amplitudes. Cells' preferred vectors were estimated by averaging the CCW and CW response phases

of the first harmonic at each temporal frequency. S-cone inputs to PC cells were estimated from the preferred vector projections in the equiluminant plane using *Eq. 1*, and S-cone inputs to MC cells were estimated from the preferred vector projections in the L+M versus S-cone plane using *Eq. 3*. L- and M-cone input ratios were estimated from the preferred vector projections in the L- versus M-cone plane using *Eq. 2*. The detailed derivation of *Eqs. 1–3* can be found in the APPENDIX

$$\frac{w_s S}{w_l L - w_m M} = \tan(\theta_{Pref(Equi)}) \quad (1)$$

$$\frac{w_m M}{w_l L} = \tan(\theta_{Pref(LM)}) \quad (2)$$

$$\frac{w_l L + w_m M}{w_s S} = \tan(\theta_{Pref(LumS)}) \quad (3)$$

In these equations, $\theta_{Pref(Equi)}$, $\theta_{Pref(LM)}$, and $\theta_{Pref(LumS)}$ are the preferred vector projections in the three planes, and w_l, w_m, and w_s are cone weights. For comparison with the DKL method, we fitted our data collected with the DKL method from the three planes simulta-

neously and found the cone weights that gave the smallest root-mean-square error, as described by Derrington et al. (1984).

RESULTS

We first show the derivation of the preferred vectors of PC, MC, and +S-(L+M) and -S+(L+M) koniocellular (KC) cells. We then consider S-cone input, and estimate the extent to which apparent S-cone input may be artifactual. Finally, we consider M- and L-cone weights for PC cells, which proved straightforward, and for MC cells, which was more complex. The physiological data sample consisted of 44 MC cells, 62 PC cells and 5 +S-(L+M) and 4 -S+(L+M) KC ganglion cells from the parafovea. For some cells complete data sets were not acquired.

Estimation of cone weights

Figure 3 shows a typical +M-L PC ganglion cell's response in the three planes. Figure 3, *A1–A3*, *B1–B3*, and *C1–C3*,
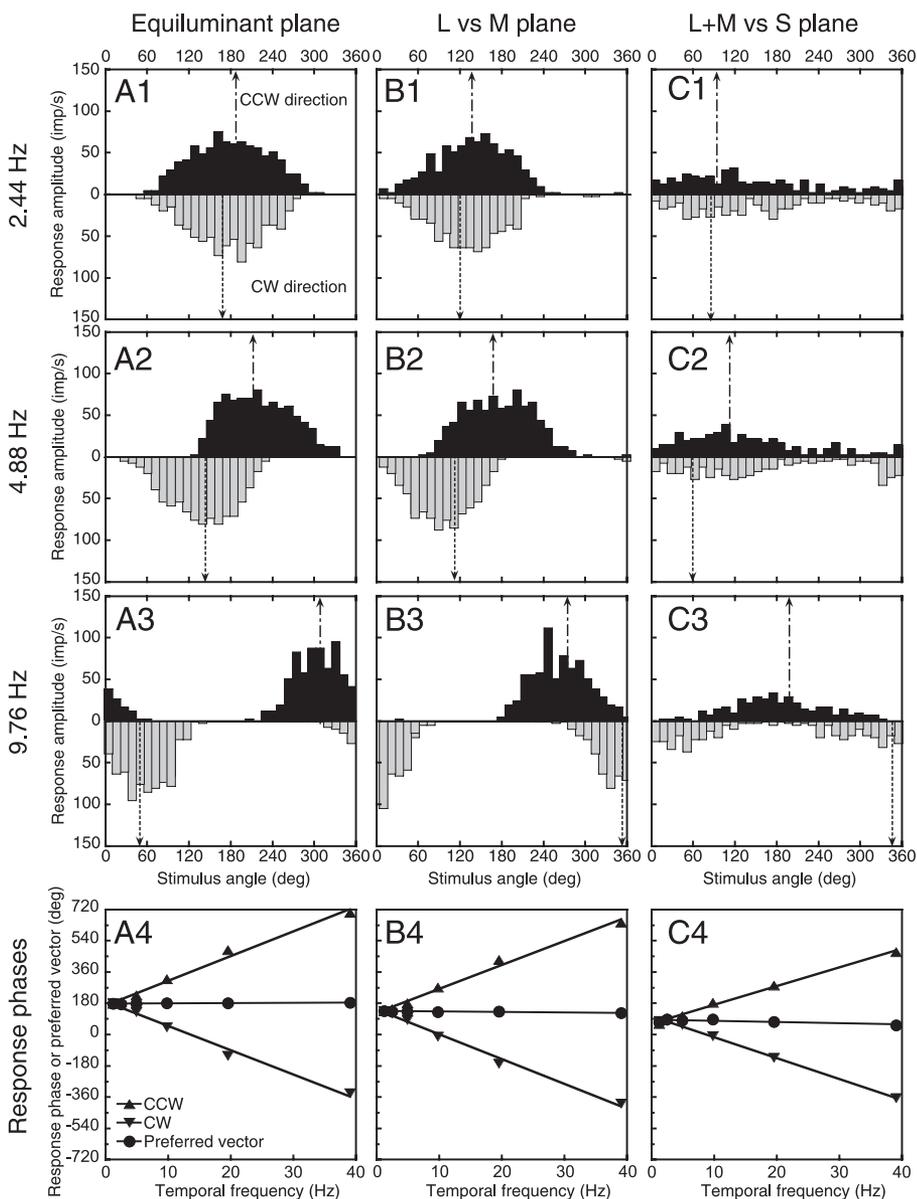

FIG. 3. Responses of a +M-L parvocellular (PC) ganglion cell. *A1–C3*: cell response histograms to CCW (black bars) and CW (gray bars) modulation in 3 color planes at 2.44, 4.88, and 9.76 Hz. CW histogram is flipped downward for comparison. *A4–C4*: cell CCW, CW response phases and preferred vectors as a function of temporal frequency. Solid lines represent linear fits.

shows the cell's response histograms to CCW (black bars) and CW (gray bars) modulation at 2.44, 4.88, and 9.76 Hz. The *x*-axis represents stimulus angle, and the *y*-axis represents response amplitude. The histogram for the CW modulation is inverted so that the two histograms can be compared. The arrows with the dotted-dashed line and the dotted line indicate the CCW and CW response phases, respectively. Figure 3, *A4–C4*, shows the cell's response phases and its preferred vectors in the three color planes as a function of temporal frequency. Solid lines represent linear fits to the response phases and the preferred vectors. At 2.44 Hz, the phase delay is small, the two histograms overlap, and the CCW and CW response phases are both close to the preferred vector. As temporal frequency increases, the phase lag increases, the histograms shift away from each other, and the CCW and CW response phases move away from the preferred vector. We performed cycle-by-cycle Fourier analysis to the spike trains and estimated 95% confidence limits of response phases at each temporal frequency. The 95% confidence limit typically ranged from 2 to 10°, which is smaller than the symbol size in Fig. 3, *A4–C4*. The response phases vary almost linearly with temporal frequency, which suggests a fixed time delay. The estimated time delay derived from the slope of the fit is ~30–45 ms, which is similar to results in the literature (Lee et al. 1994). The average of the CCW and CW response phases, the cell's preferred vector, did not change significantly with temporal frequency. This was the case for most PC cells. Cone weights can be calculated from the preferred vector using *Eqs. 1* and *2*. For this PC cell, the preferred vector for the equiluminant plane is 177.0° and for the L+M and S plane is 85.2°, which would indicate an S-cone input equivalent to 3.4% of the L-M signal; the mean vector for the L- versus M-cone plane is 135.2°, which indicates a balanced L-, M-cone opponent input. The behavior of most PC cells followed the patterns shown in Fig. 3.

Figure 4 shows an ON-center MC ganglion cell's response in the L- versus M-cone plane (*A1–A4*) and in the L+M versus S-cone planes (*B1–B4*). The MC cell gave little first-harmonic response to modulation in the equiluminant plane, and data are not shown. Otherwise the format is the same as in Fig. 3. At low frequencies, the cell's responses were phase-advanced as expected of cells with transient responses, and the CCW and CW response phases cross. As temporal frequency increases, the cell's CCW and CW response histograms move away from each other because of the phase delay. The MC cell's response phases vary approximately linearly with temporal frequency. The average of CW and CCW response phases again predicts the cell's preferred vector, and it does not change with temporal frequency. Cone weights can be calculated using *Eqs. 2* and *3*. For this MC cell, the preferred vector for the L- versus M-cone plane is 34.5°, which suggests an L to M ratio of 1.4:1, and the preferred vector for the L+M and S-cone plane is 85.6°, which indicates an S-cone input equivalent to 3.0% of the L+M signal. In the next section, we examine the extent to which this may be caused by variation in prereceptoral filtering. Some MC cells showed more complex response properties for modulation in the L- and M-cone plane. The preferred vector was in the chromatic quadrant at lower temporal frequencies and in the luminance quadrant at higher temporal
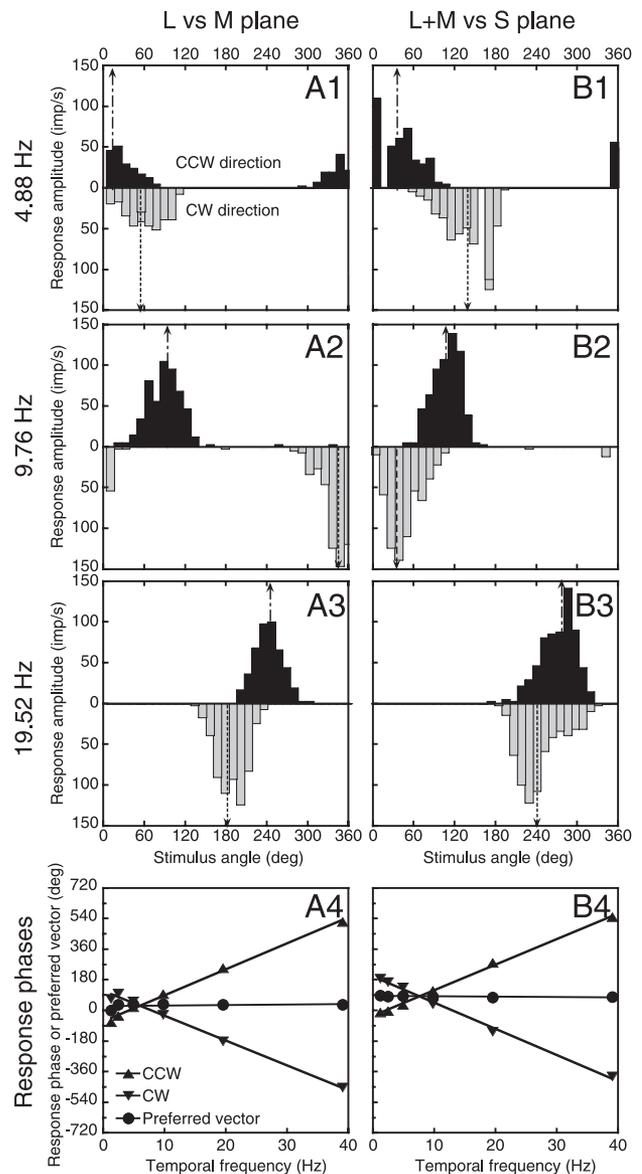

FIG. 4. Responses of an ON-center magnocellular (MC) ganglion cell. *A1–B3*: cell response histograms to CCW and CW modulation in the L- vs. M-cone plane and L+M vs. S-cone planes at 4.88, 9.76, and 19.52 Hz. The cell gave little response to modulation in the equiluminant plane; these data are not shown. *A4* and *B4*: cell response phases and preferred vectors as a function of temporal frequency. Format is the same as in Fig. 3.

frequencies (Fig. 9). This is consistent with previous reports of a first-harmonic chromatic response in MC cells at low temporal frequencies (Lee et al. 1993; Smith et al. 1992).

Figure 5 shows a typical +S-(L+M) ganglion cell's response in the three color planes. The format is the same as in Fig. 3. The preferred vector for the equiluminant plane is 84.7°, which indicates predominantly S-cone input with little L-M opponent signal; the preferred vector for the L- versus M-cone plane is 226.6°, which indicates an inhibitory L+M input; the preferred vector for the L+M versus S-cone plane is 333.5°.

First-harmonic response amplitudes as a function of temporal frequency were consistent with estimates in the literature (Lee et al. 1990), i.e., PC cells' response curves were usually low-pass (sustained) and those of MC cells were band-pass (transient). Stimulus contrasts had been selected to evoke
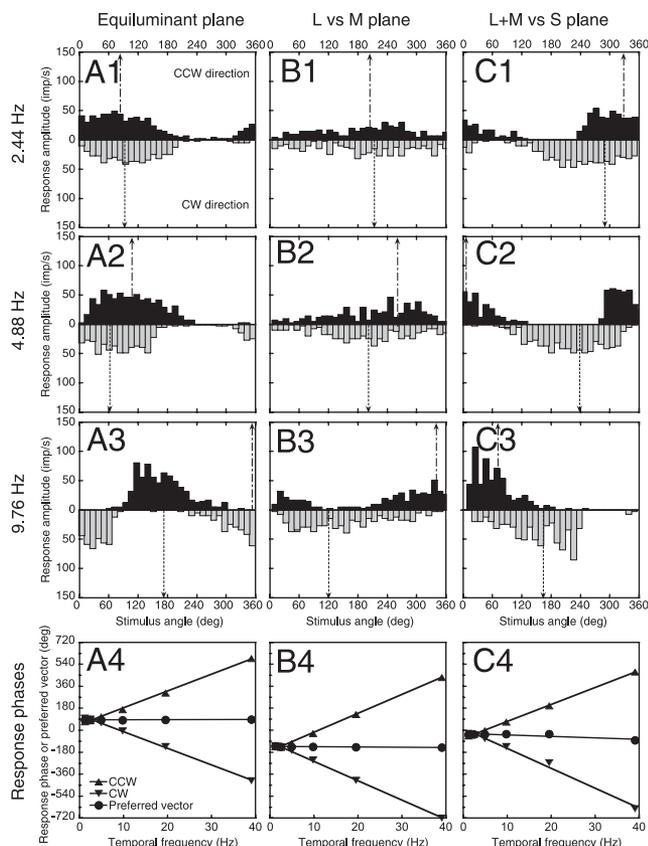
FIG. 5. Responses of a +S-(L+M) koniocellular (KC) ganglion cell. *A1–C3*: cell response histograms to CCW and CW modulation in the 3 color planes at 3 temporal frequencies. *A4–C4*: cell response phases and preferred vectors as a function of temporal frequency. Format is the same as in Fig. 3.

vigorous responses under the conditions tested, but in a few instances (predominantly at high frequencies), response amplitudes fell below 5 impulse/s, and the data were discarded. There is evidence that MC cells receive both an L-, M-cone additive input and an L-, M-cone opponent input at low temporal frequencies (Smith et al. 1992). If these inputs have different phase delays, response amplitude may depend on the direction of rotation and response phase behavior may become more complex (see DISCUSSION).

Strength of S-cone inputs

We used the new method to test S-cone inputs to PC and MC cells. S-cone inputs to PC ganglion cells can be estimated from PC cells' preferred vector projections in the equiluminant plane. In Fig. 6, *A1* shows the distribution of PC cells' preferred vectors. They cluster around 0 and 180° for +L-M and +M-L cells, respectively. The ratio of S-cone input to L-M input can be calculated for each cell from the preferred vectors in the equiluminant plane. The distribution is shown in Fig. 6*A2*. It clusters around zero, but there is some variability. Similarly, for MC cells, the amount of S-cone input can be estimated from MC cells' preferred vectors in the L+M versus S-cone plane. Figure 6*B1* shows the distribution of MC cells' preferred vectors in this plane. They cluster around +90 and −90° for ON-and OFF-center cells, respectively. The ratio of S-cone input to L+M input can be calculated from the pre-

ferred vectors using *Eq. 3* and is shown in Fig. 6*B2*. Values vary around zero.

We used the Smith-Pokorny transformation applied to the CIE 1964 10° color matching functions and the 10° V_λ luminosity function in our calibration. If this calibration is not strictly appropriate for the macaque or if there is variation in prereceptoral filtering because of interanimal variability or variation in eccentricity, or other experimental factors, this will be reflected as variation in cells' preferred vectors. Therefore in a control experiment, we repeated the measurements at different S-cone adaptation levels. We varied the mean chromaticity away from EEW along a tritanopic confusion line to increase S-cone adaptation, i.e., the whole modulation circle was displaced along the +S axis in the equiluminant plane (for PC cells) and in the L+M versus S-cone plane (for MC cells).

Figure 7 shows S-cone adaptation results. If a neuron receives actual S-cone input, as in the case of a +S-(L+M) ganglion cell, the cell's preferred vector should vary with the level of S-cone adaptation at all temporal frequencies as the S-cone relative weight decreases because of adaptation. This is shown in Fig. 7*A1*. The triangles represent the +S-(L+M) cell's preferred vectors in the L+M versus S-cone plane for different temporal frequencies and different S-cone adaptation levels. Dashed lines represent linear fits. The preferred vector of the cell varied with S-cone adaptation level with a slope of 12.1° per unit of mean S-cone adaptation, consistent with a decrease in effective S-cone weight. On average, +S-(L+M) cells' response amplitude decreased to 35% of the mean response amplitude (SE, 1.9%) when the S-cone adaptation increased to four times the mean level. This indicates a degree of adaptation falling somewhat short of Weber's law, similar to the S-cone adaptation properties in outer retina (Lee et al. 1999).

If a cell receives only L- and M-cone input and no S-cone input, the cell's preferred vector would not vary with the level of S-cone adaptation. This is shown by the preferred vectors of a +L-M PC in the equiluminant plane and of an ON-center MC cell in the L+M versus S-cone plane (Fig. 7, *A2* and *A3*). The preferred vectors were not exactly 0 or 90° for the two cells, suggesting possible S-cone input. However, they showed no systematic variation with the level of S-cone adaptation, indicating that the putative S-cone input was artifactual. This was the case for most PC and MC cells. After combining data across different temporal frequencies, we fitted the S-cone adaptation curve with a linear function. The distribution of the slopes of the linear fits for PC and MC cells are shown in Figs. 7, *B1* and *B2*. They are tightly clustered around a slope of 0.0. 75% of PC, and 90% of MC cells had slopes not significantly different from 0.0 ($P > 0.05$). The average slope (without signs) for the remaining 25% of PC cells and 10% of MC cells is ~1.2° per multiple of mean S-cone adaptation.

Figure 7 suggests that the deviation of MC and PC cells' preferred vectors from −90 and +90° (MC) and 0 and 180° (PC) is caused by factors other than S-cone input. If the S cones are largely adapted at the maximal S-cone adaptation level, any apparent S-cone input that remains is an estimate of this artifact. By subtracting the S-cone inputs at maximal S-cone adaptation from those at the EEW condition, we can discount the artifact to estimate the actual S-cone input to ganglion cells. Figure 6, *A2–A4*, shows the S-cone inputs to PC cells estimated at EEW, the maximal S-cone adaptation level,
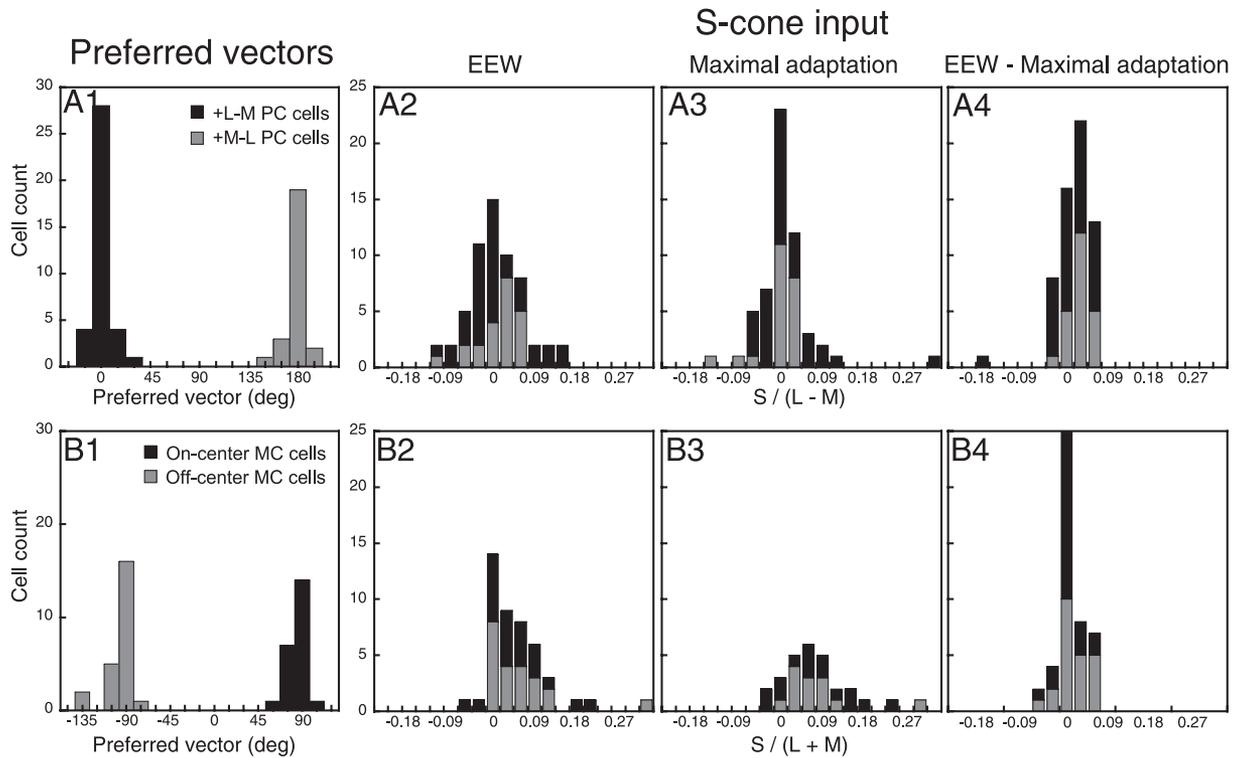
S-cone input

Preferred vectors

FIG. 6. Distribution of PC and MC cells' preferred vectors and estimated S-cone inputs. *A1*: distribution of PC cells' preferred vectors in the equiluminant plane. *B1*: distribution of MC cells' preferred vectors in the L+M vs. S-cone plane. *A2–A4* and *B2–B4*: estimated S-cone inputs based on cells' preferred vectors at equal energy spectrum white (EEW), maximal S-cone adaptation, and difference between the 2 conditions. Dark and gray bars represent +L-M and +M-L PC cells, or ON-center and OFF-center MC cells.

and the difference between the two. Figure 6, *B2–B4,* shows similar data for MC cells. The narrowing of S-cone distribution after subtraction (Fig. 6, *A4* and *B4*) compared with EEW condition (Fig. 6, *A2* and *B2*) suggests that most of the scatter

of PC and MC cells' preferred vectors is unlikely to be caused by S-cone input. For both cell classes, the mean S-cone inputs (calculated after performing the subtraction) do not differ significantly from 0.0 ($P > 0.5$).
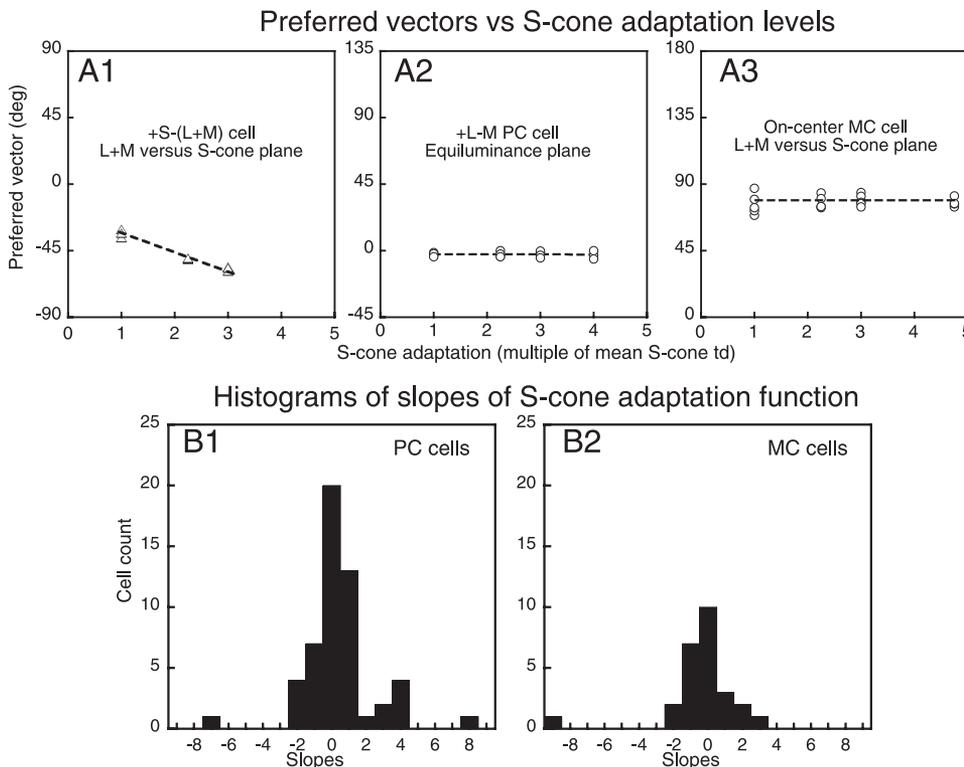
FIG. 7. S-cone adaptation. *A1–A3*: preferred vectors at different S-cone adaptation levels for a +L-M PC cell (*A2*) in the equiluminant plane, an ON-center MC cell (*A3*) and a +S-(L+M) KC cell (*A1*) in the L+M vs. S-cone plane. The +S-(L+M) cell gave little response at maximal S-cone adaptation level. The preferred vector of the +S-(L+M) cell varies clearly with S-cone adaptation level, whereas those of PC and MC cells show little or no variation. *B1* and *B2*: distribution of slopes of the S-cone adaptation function for all PC and MC cells. They cluster around 0.

FIG. 8. Distribution of M- to L-cone input ratio for PC and MC cells. Dark and gray bars represent data for +L-M and +M-L PC cells, or ON- and OFF-center MC cells, respectively.

L- and M-cone inputs

The ratio of L- and M-cone inputs to MC and PC ganglion cells can be estimated from the ganglion cells' preferred vectors in the L- versus M-cone plane using *Eq 2*. This is straightforward for PC cells. There was no systematic change in preferred vectors, i.e., relative L- to M-cone weights, with temporal frequency, in agreement with earlier measurements (Smith et al. 1992). We either a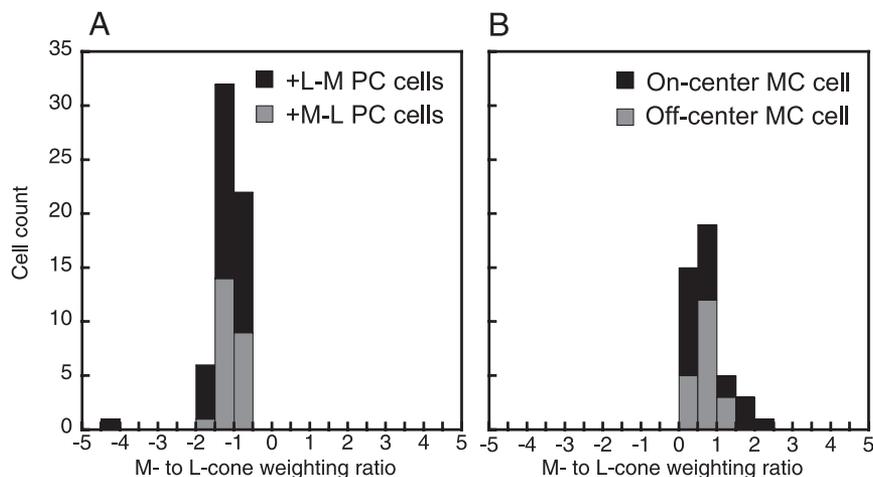veraged preferred vectors over temporal frequency or extrapolated the linear fit of the preferred vectors to 0 Hz to estimate L- and M-cone weights. Both calculations yielded very similar results. Figure 8*A* shows the histogram of the estimated M- to L-cone weights for PC cells. The relative weights cluster around ~1.0, suggesting that most PC cells have balanced L- and M-cone opponent inputs for our conditions of adaptation. This is consistent with data from the literature (Derrington et al. 1984; Lee et al. 1987).

The situation is more complicated for MC cells. They appear to receive opponent as well as additive L-, M-cone inputs at low temporal frequencies (Lee and Sun 2004; Smith et al. 1992), which may correspond to the original observation of Wiesel and Hubel that MC cells were inhibited when their surrounds were "flooded with red light" (Wiesel and Hubel 1966). The additive input becomes dominant above 10 Hz. An example of such a cell is shown in Fig. 9. The preferred vector in the L- versus M-cone plane changes with temporal frequency, being in the L-, M-cone opponent quadrant (307 or −53°) for 1.22 to 4.88 Hz, but shifting to the L-, M-cone additive quadrant (208 or −152°) at higher temporal frequencies. We averaged the preferred vector fits at the two highest temporal frequencies, 19.52 and 39.04 Hz, to estimate the ratio of L- and M-cone weights of the achromatic input. The ratio of M- to L-cone weights for MC cells clustered around a median value of 0.6 (Fig. 8*B*). This is consistent with the 1.5:1 ratio of L- to M-cone sensitivities in the human luminosity function. The distribution of MC cells' cone ratios is broader than that of PC cells, which suggests a larger variation of L- and M-cone weights for MC cells. One MC cell was M-cone dominant with a M- to L-cone ratio of 18.0, and is not shown in Fig. 8*B*.

Comparison of cone weights estimated with the DKL method

To compare with the results of the new method, cone inputs were also estimated using the DKL technique. We measured

ganglion cells' responses to modulation along lines of various orientations through the EEW point in the three color planes at 3.26 and 19.52 Hz, and fitted the cells' response amplitudes with a linear model that has three free parameters, the relative S-, M- and L-cone weights and a scaling factor. A comparison of estimated cone weights using the two methods is shown in Figs. 10 and 11. Derrington et al. used a temporal modulation of 3.75 Hz for both MC and PC cells, whereas we used 3.26 Hz DKL data for PC cells and 19.52 Hz DKL data for MC cells in the comparison to minimize the effect of PC cells' center-surround latency and MC cells' chromatic responses.

Figure 10 shows results plotted in the cone weighting space described by Derrington et al. (1984). Symbols plotted on the diagonal line segments, $|x| + |y| = 1$, represent cells with solely M- and L-cone inputs, while those falling inside the diamond also receive S-cone input. Cells that receive additive L-, M-cone inputs, such as MC, and +S-(L+M) and -S+(L+M) KC cells, fall in the first and third quadrants, whereas cells that receive opponent L-, M-cone inputs, such as PC cells, fall in the second and fourth quadrants. With our method (Fig. 10*A*), PC cells fall along the line segments and cluster closely around the midpoints, (−0.5, +0.5) and (+0.5, −0.5), indicating balanced L-, M-cone weights with little S-cone input. With the DKL method (Fig. 10*B*), PC cells showed relatively larger variation with more cells falling inside the square. Results similar to ours were also obtained by Reid and Shapley (2002) for PC and KC cells in the LGN.

Figure 11 shows the cone weights estimated from the two methods plotted against each other. The *x*- and *y*-axis represent estimates using our method and the DKL method, respectively. Each symbol represents an individual cell. For the estimates of M- to L-cone ratio, the two methods give similar means for both MC and PC cells, but the variation of M- to L-cone ratio for PC cells is smaller with our method than with the DKL method. For the estimates of S-cone input, both the mean and variation are smaller with our method than with DKL method. This is partly because, with our method, we repeated measurements at higher S-cone adaptation levels, which was expected to reduce artifactual S-cone input because of variations in prereceptoral filtering.

In summary, the results show that the method described here is effective and accurate at assessing weights and signs of cone inputs to visual neurons. It does not require linearity of a
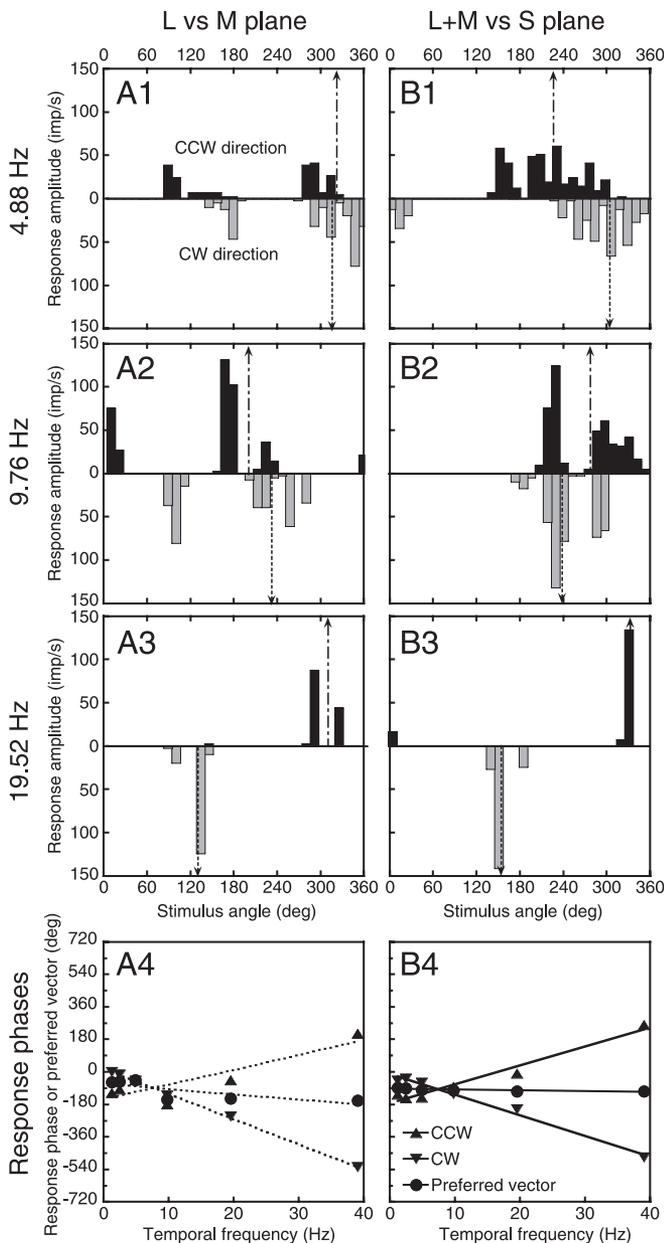
FIG. 9. Responses of an OFF-center MC ganglion cell. Format is similar to Fig. 4. For modulation in the L- vs. M-cone plane, the cell's preferred vector was in the opponent quadrant at low frequency but moved to the achromatic quadrant at higher frequencies. Linear fit for preferred vectors in this plane (dashed line) is drawn only to show the nonzero slope.

neuron provided that the majority of energy in the neuron's response is in the first harmonic. Higher harmonic components do not affect the estimate of the cell's preferred vector. The method does require that cells show modulated responses to the stimuli; otherwise, phase information cannot be obtained.

DISCUSSION

Comparison of different methods

We introduce a rapid and precise method to measure weights and signs of cone inputs to visual neurons. There are three other published methods for estimation of cone weights (Derrington et al. 1984; DeValois et al. 1966; Johnson et al. 2004;

Reid and Shapley 2002). The original method of measuring cell responses to pulses of single wavelength (DeValois et al. 1966) had a number of drawbacks, including a lack of control of adaptation state. Derrington et al. (1984) estimated cells' null planes by measuring response amplitude to modulation along lines of various orientations in three planes of a 3-D color space. Our method is, in a sense, an efficient version of the DKL method, because each circle of modulation simultaneously contains all the individual DKL modulations through the origin in a single plane. Measuring responses to CW and CCW modulation requires fewer measurements than modulation along lines of a large number of orientations in the DKL technique. For example, it is fourfold faster than the DKL method when the DKL measurement includes eight orientations at a stepsize of 22.5°. The increased efficiency of our method enables us to measure the complete cone weighting for each cell at different temporal frequencies and in different states of adaptation. In addition, measuring response phase allows accurate angular resolution of the preferred vector in each plane; the cycle-to-cycle estimation of response phase showed 90% CIs of 2–10°. In another method, Reid and Shapley (2002) and Johnson et al. (2004) estimated cone weights by measuring a cell's response to L-, M-, and S-cone isolating modulation. This is a simplified version of the DKL method. It provides estimates of the relative cone weights by assuming the cone signals are linearly combined. Additional measurements to combinations of cone modulations would be needed to separate linear from nonlinear cells.

Our method does not require strict linearity of neurons; cell responses can be modulated by nonlinear mechanisms without affecting the analysis, provided the response is dominated by the first harmonic and there are no severe nonlinearities of cone combination. The DKL technique estimates cone weights by fitting cells' response amplitudes with linear weighting functions, and the high luminance contrast used in the original study could cause response distortion caused by contrast saturation. Reid et al. and Johnson et al. estimated cone weights from cells' response amplitude to cone isolating stimuli directly, and they avoided response saturation by restricting the stimulus to low contrast. Our method is relatively more robust to response saturation and phase changes caused by contrast gain control because phase changes from these sources will be eliminated by averaging over CW and CCW modulation. In addition, our method, based on response phase, may be less susceptible to drifts in responsivity and higher harmonic distortions. Drifts in responsivity between measurements along different axes could influence the estimate of the preferred vector, but this effect should be minimized in our method because all the linear modulations in the DKL method are present in each circular modulation.

The technique used in this paper is optimal for ganglion cells and LGN cells which respond to full-field modulation. Cortical cells that have elongated receptive fields and do not respond to full-field modulation can be studied by using "rainbow" gratings, i.e., gratings of which the color varies through a complete color circle. Analogous to our temporal stimuli, rainbow gratings are phase-shifted sums of the sinusoidal gratings along color axes used by Lennie et al. (1990) and Gegenfurtner et al. (1994). Response phases of simple cells to moving rainbow gratings could be used to infer cone weights. For complex cells
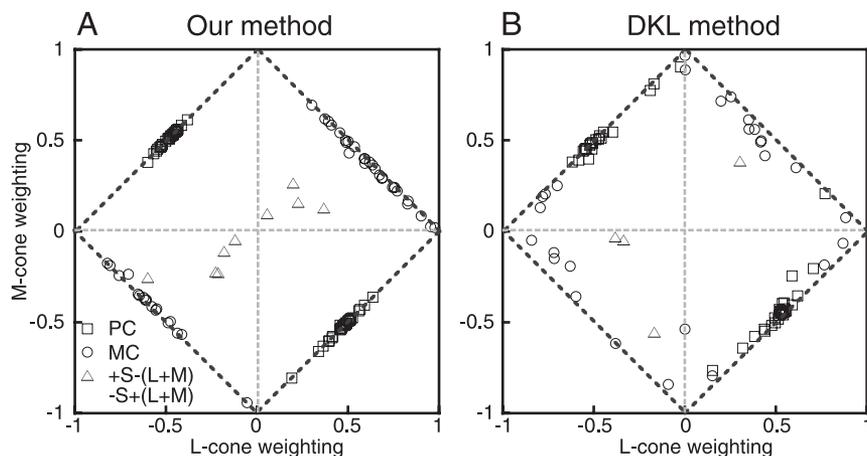
FIG. 10.   Comparison of cone weights assessed with our method and the Derrington, Krauskopf, and Lennie (DKL) method. Cone inputs are shown in cone weighting space. Cells plotted on diagonal line segments are those with solely M- and L-cone inputs, whereas those falling inside the square receive S-cone input.

that respond by phase-independent changes in mean firing rates, such gratings would not be useful.

To infer the ratio of L-, M-, and S-cone input from the cell's preferred vector, we assumed that the phase delays for L-, M-, and S-cone modulation are similar: $\theta_l(f) \approx \theta_m(f) \approx \theta_s(f)$. This is approximately the case (Yeh et al. 1995). However, for PC ganglion cells, there is a center-surround latency difference of 2–4 ms (Lankheet et al. 1998; Lee et al. 1993; Smith et al. 1992), which translates to a phase difference between L- and M-cone mechanisms of about 1°/Hz. We calculated the effect of such a delay on preferred vectors (Fig. 12). It is very small at temporal frequencies ≤20 Hz, but can become significant at

40 Hz, causing an underestimate of the weaker cone input of ≤10% of the measured value. However, systematic changes in cone weight with frequency were extremely rare for PC cells, which suggests that *Eqs. 1–3* remain a good approximation.

S-cone inputs

The human luminosity function is generally modeled as the sum of M- and L-cone sensitivities (Smith and Pokorny 1972); an S-cone contribution is not required. Even in studies where some S-cone input is allowed (Vos and Walraven 1971), the contribution of the S-cone is very small, of the order of 1%.
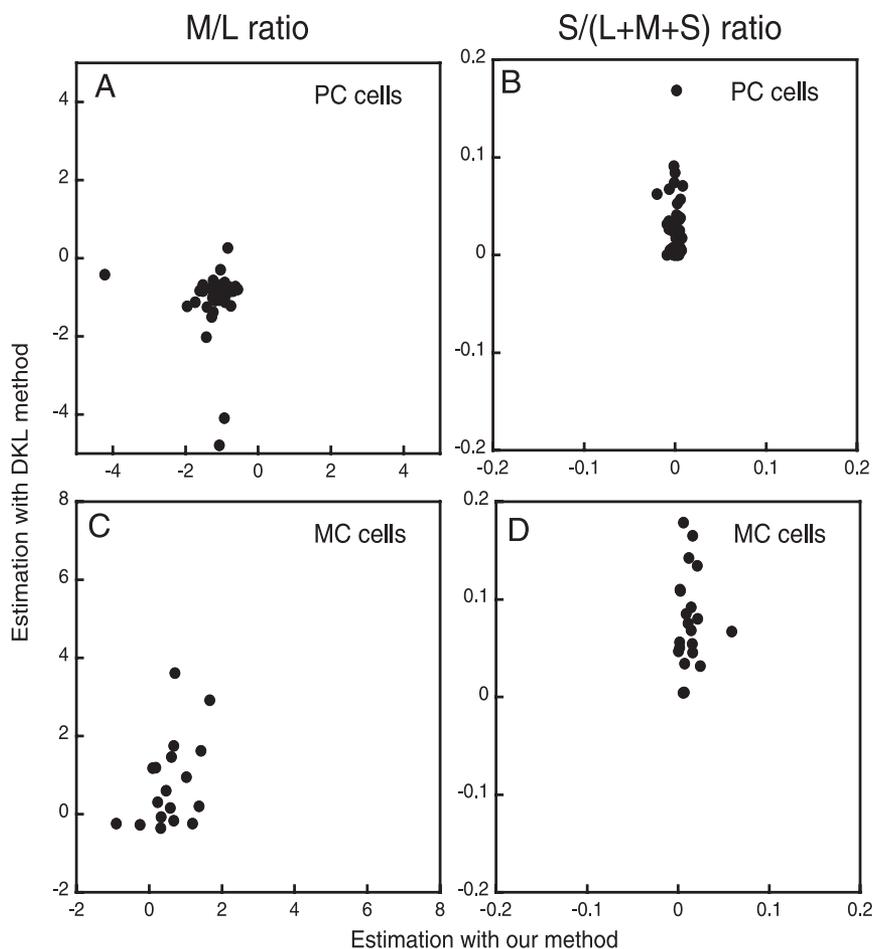
FIG. 11.   Comparison between our method and the DKL method for individual cells. Ratio of M-, L-, and S-cone weights from the 2 methods are plotted against each other. Each symbol represents data from an individual cell. For the DKL method, 3.26-Hz PC cell data and 19.52-Hz MC cell data were used.
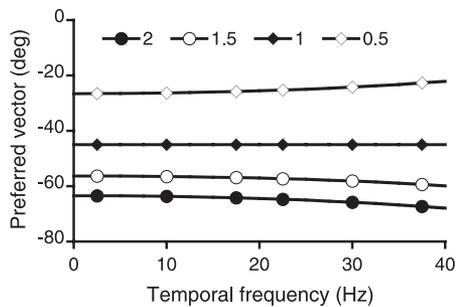
FIG. 12. Effect of phase difference between $\theta_l(f)$ and $\theta_m(f)$ on preferred vectors for the L- vs. M-cone plane. Model simulation is for a PC cell with various M- to L-cone ratios. Phase lag between $\theta_l(f)$ and $\theta_m(f)$ is 3 ms. When M- and L-cone inputs are balanced, phase lag has no effect on the cell's preferred vector. When M- and L-cone input are not balanced, the cell's preferred vector shifts by 5° at 40 Hz.

This is further supported by psychophysical evidence from flicker photometry, minimum motion, and minimally distinct border studies (Cavanagh et al. 1987; Eisner and MacLeod 1980; Smith and Pokorny 1975; Tansley and Boynton 1976; Valberg and Tansley 1977). MC cells show properties that strongly suggest they form the physiological substrate of the luminance channel (Kaiser et al. 1990; Lee et al. 1988).

An identification of a psychophysical luminance channel with the MC pathway appears at odds with the results of Chatterjee and Callaway, who found 7% S-cone input to MC cells in the LGN (Chatterjee and Callaway 2002). A potential reason for this discrepancy stems from their calculation of S-cone isolating stimuli. We calibrated our stimuli with the 10° V_λ luminosity function (Shapiro et al. 1996) for measurements in the parafovea, as did Derrington et al. and Johnson et al., whereas Chatterjee and Callaway calculated their stimuli with the 2° V_λ luminosity function for measurements in the parafovea. The major difference between the two luminosity functions is the absence of macular pigment in the 10° V_λ function. Macular pigment is present only in the fovea and has its peak absorption at short wavelengths. We calculated that the failure to correct for lack of macular pigment would lead to ~6% residual luminance contrast in the putative S-cone isolating stimulus (for stimuli similar to those used by Chatterjee et al.). For purposes of comparison, we carried out a series of measurements using the 2° cone fundamentals, and these resulted in a spurious S-cone weighting of 6–8%.

Chatterjee and Callaway used a strongly adapting yellow background (generated with a Kodak Warren 15 filter that passes lights of wavelength 530 nm or longer) as a control, which may have revealed some S-cone input, but under such conditions psychophysical studies provide evidence for a weak S-cone influence on flicker nulls (Stockman et al. 1991, 1993). On the other hand, the yellow adapting background contains long-wavelength lights, which differentially adapt L-cones in a non-Weberian manner, leaving M-cone contributions to the luminance channel less affected (Eisner and MacLeod 1981). We calculated that the residual M-cone contrast in the putative S-cone isolating stimulus was ~18%, whereas the L-cone contrast was ~4%. Both these factors could contribute to the residual response on the yellow background.

Specificity of retinal wiring

The lack of S-cone signals to PC and MC ganglion cells has anatomical significance. In the central 10° of retina, a single midget bipolar cell connects to a single L or M cone, which in turn connects exclusively to a single midget ganglion cell. This wiring would exclude S-cone input through the center, so any S-cone input would be anticipated to be from the surround. It is currently debated whether midget ganglion cells derive surround inputs randomly from the cone mosaic or from just L or M cones (Lee et al. 1998; Lennie et al. 1991; Mullen and Kingdom 1996; Reid and Shapley 1992, 2002). S cones make up 8–10% of the cone population in the parafovea (Martin and Grünert 1999). If the random wiring scheme is true, one might expect a mean S-cone input of 8–10% with a sign the same as for the surround. For PC cells (see Fig. 6), we did not find any suggestion that possible S cone inputs had the same sign as the surround. For MC cells, the center dominates the flicker response, and so most S-cone input would be expected to be of the same polarity as the center. Comparing ON- and OFF-center MC cells showed no effect of this sort. Parasol ganglion cells construct their centers from diffuse bipolar cells, of which there are six types (Boycott and Wässle 1991). Cone selectivity has only been studied anatomically for one type, the DB6 (Lee et al. 2004), which shows no selectivity. The presence or absence of S-cone contacts is unknown for the other types, but there is a precedent for selective avoidance of S-cone input in outer retina; the H1 horizontal cell makes very few S-cone contacts (Dacey et al. 1996). In any event, the lack of demonstrable S-cone input to both ganglion cell types implies some underlying connectional specificity. The locus of this specificity is yet unknown. We do not imply, however, that S-cone input is totally absent (even the H1 horizontal cell makes occasional S-cone contacts), but that it is functionally undetectable under our conditions of adaptation.

The exclusion of S-cone input to the MC and PC pathways may have functional significance. Efficient information transmission in the retinal output is achieved by linear operators with the least possible correlation (Buchsbaum and Gottschalk 1983). The absence of S-cone input to the L-M system leads to the least possible correlation with the S-(L+M) system. In addition, isolating the L-M system from S-cone inputs makes it more useful for detecting reddish-yellowish fruit against greenish foliage (Parraga et al. 2002). In a single scene, the colors of leaves differ primarily because of their angles to the sun. Their color variation is thus along the yellowish-bluish color axis between sunlight and skylight (Taylor and Kerr 1941), and the absence of S-cone input means that this variation does not provide distracting noise to the L-M system. In addition, lack of S-cone input may arise because S-cone signals can be spatially degraded because of chromatic aberration at short wavelengths, which may make such inputs disadvantageous for high spatial frequency systems.

The results of this paper show that preferred color directions of ganglion cells fall into a very small number of classes. In the striate cortex, however, preferred vectors do not cluster around particular directions in either the equiluminant plane or the luminance-chromaticity planes (Johnson et al. 2001; Lennie et al. 1990). For analysis of a colorful environment, linear cone projections thus give way to analyzers with more specific ability to analyze patterns. It is possible that having a discrete

number of classes of linear, uncorrelated inputs makes it easier to form systems of pattern-matching color neurons for each retinotopic location.

APPENDIX

In this section, we show that the preferred vector θ_{Pref}, which is determined by the cone weights, can be estimated by the average of the CCW response phase θ_{CCW} and CW response phase θ_{CW}.

When a stimulus is modulated around a circle in a color plane in the CCW direction at temporal frequency f, the variation of L-, M-, and S-cones from the EEW point can be written as

$$L \cos(2\pi ft - \psi_{\text{l}}) \qquad (4)$$

$$M \cos(2\pi ft - \psi_{\text{m}}) \qquad (5)$$

$$S \cos(2\pi ft - \psi_{\text{s}}) \qquad (6)$$

where L, M, S are the L-, M-, and S-cone modulation amplitudes, ψ_{l}, ψ_{m}, and ψ_{s} are the azimuth of the L-, M-, and S-cone axis in radians, f is the temporal frequency in radians per second, and t is time in seconds. A ganglion cell's response to isolated L-, M-, and S-cone modulation can be written as

$$R_{\text{l}}(t) = w_{\text{l}}L \cos[2\pi ft - \psi_{\text{l}} - \theta_{\text{l}}(f)] = W_{\text{l}} \cos[2\pi ft - \psi_{\text{l}} - \theta_{\text{l}}(f)] \qquad (7)$$

$$R_{\text{m}}(t) = w_{\text{m}}M \cos[2\pi ft - \psi_{\text{m}} - \theta_{\text{m}}(f)] = W_{\text{m}} \cos[2\pi ft - \psi_{\text{m}} - \theta_{\text{m}}(f)] \qquad (8)$$

$$R_{\text{s}}(t) = w_{\text{s}}S \cos[2\pi ft - \psi_{\text{s}} - \theta_{\text{s}}(f)] = W_{\text{s}} \cos[2\pi ft - \psi_{\text{s}} - \theta_{\text{s}}(f)] \qquad (9)$$

where w_{l}, w_{m}, and w_{s} are cone input weights, and $\theta_{\text{l}}(f)$, $\theta_{\text{m}}(f)$, and $\theta_{\text{s}}(f)$ are the ganglion cell's response phase to L-, M-, and S-cone modulation, which include delays of cone responses within the cones themselves and any delays that follow the second-stage cone combination. $W_{\text{l}} = w_{\text{l}}L$, $W_{\text{m}} = w_{\text{m}}M$, $W_{\text{s}} = w_{\text{s}}S$. The cone weights include gain control of cone responses and synaptic efficiency between cone and ganglion cells. The ganglion cell's response to the CCW modulation equals $R_{\text{l}}(t) + R_{\text{m}}(t) + R_{\text{s}}(t)$, which is also a sinusoidal modulation

$$R_{\text{ccw}} = A_{\text{ccw}} \cos[2\pi ft - \theta_{\text{ccw}}(f)] = W_{\text{l}} \cos[2\pi ft - \psi_{\text{l}} - \theta_{\text{l}}(f)]$$
$$+ W_{\text{m}} \cos[2\pi ft - \psi_{\text{m}} - \theta_{\text{m}}(f)] + W_{\text{s}} \cos[2\pi ft - \psi_{\text{s}} - \theta_{\text{s}}(f)] \qquad (10)$$

where A_{CCW} and $\theta_{\text{CCW}}(f)$ are the amplitude and phase of the ganglion cell's response.

The term of primary interest is the response phase $\theta_{\text{CCW}}(f)$. We can derive $\cos[\theta_{\text{CCW}}(f)]$, $\sin[\theta_{\text{CCW}}(f)]$, and hence $\tan[\theta_{\text{CCW}}(f)]$ by setting $2\pi ft$ to 0 and $\dfrac{\pi}{2}$ in Eq. 10

$$\tan[\theta_{\text{ccw}}(f)] =$$
$$\frac{W_{\text{l}} \sin[\theta_{\text{l}}(f) + \psi_{\text{l}}] + W_{\text{m}} \sin[\theta_{\text{m}}(f) + \psi_{\text{m}}] + W_{\text{s}} \sin[\theta_{\text{s}}(f) + \psi_{\text{s}}]}{W_{\text{l}} \cos[\theta_{\text{l}}(f) + \psi_{\text{l}}] + W_{\text{m}} \cos[\theta_{\text{m}}(f) + \psi_{\text{m}}] + W_{\text{s}} \cos[\theta_{\text{s}}(f) + \psi_{\text{s}}]} \qquad (11)$$

Similarly, for a stimulus that is modulated in the CW direction

$$R_{\text{cw}} = A_{\text{cw}} \cos[-2\pi ft - \theta_{\text{cw}}(f)] = W_{\text{l}} \cos[-2\pi ft - \psi_{\text{l}} + \theta_{\text{l}}(f)]$$
$$+ W_{\text{m}} \cos[-2\pi ft - \psi_{\text{m}} + \theta_{\text{m}}(f)] + W_{\text{s}} \cos[-2\pi ft - \psi_{\text{s}} + \theta_{\text{s}}(f)] \qquad (12)$$

$$\tan[\theta_{\text{cw}}(f)] =$$
$$-\frac{W_{\text{l}} \sin[\theta_{\text{l}}(f) - \psi_{\text{l}}] + W_{\text{m}} \sin[\theta_{\text{m}}(f) - \psi_{\text{m}}] + W_{\text{s}} \sin[\theta_{\text{s}}(f) - \psi_{\text{s}}]}{W_{\text{l}} \cos[\theta_{\text{l}}(f) - \psi_{\text{l}}] + W_{\text{m}} \cos[\theta_{\text{m}}(f) - \psi_{\text{m}}] + W_{\text{s}} \cos[\theta_{\text{s}}(f) - \psi_{\text{s}}]} \qquad (13)$$

Now we can apply Eqs. 11 and 13 to each of the three color planes. For the equiluminant plane, $\psi_{\text{l}} = 0$, $\psi_{\text{m}} = \pi$, $\psi_{\text{s}} = \pi/2$, therefore

$$\tan[\theta_{\text{ccw}}(f)] = \frac{W_{\text{l}} \sin[\theta_{\text{l}}(f)] - W_{\text{m}} \sin[\theta_{\text{m}}(f)] + W_{\text{s}} \cos[\theta_{\text{s}}(f)]}{W_{\text{l}} \cos[\theta_{\text{l}}(f)] - W_{\text{m}} \cos[\theta_{\text{m}}(f)] - W_{\text{s}} \sin[\theta_{\text{s}}(f)]} \qquad (14)$$

$$\tan[\theta_{\text{cw}}(f)] = \frac{-W_{\text{l}} \sin[\theta_{\text{l}}(f)] + W_{\text{m}} \sin[\theta_{\text{m}}(f)] + W_{\text{s}} \cos[\theta_{\text{s}}(f)]}{W_{\text{l}} \cos[\theta_{\text{l}}(f)] - W_{\text{m}} \cos[\theta_{\text{m}}(f)] + W_{\text{s}} \sin[\theta_{\text{s}}(f)]} \qquad (15)$$

Projection of a cell's preferred vector in this plane is determined by its cone weights

$$\tan(\theta_{\text{Pref(Equi)}}) = \frac{W_{\text{s}}}{W_{\text{l}} - W_{\text{m}}} \qquad (16)$$

If the response phases to L-, M-, and S-cones are similar $\theta_{\text{l}}(f) \approx \theta_{\text{m}}(f) \approx \theta_{\text{s}}(f)$, the preferred vector can be estimated by the average of CCW and CW response phases

$$\tan(2\theta_{\text{Pref(Equi)}}) = \frac{2\dfrac{W_{\text{s}}}{W_{\text{l}} - W_{\text{m}}}}{1 - \left(\dfrac{W_{\text{s}}}{W_{\text{l}} - W_{\text{m}}}\right)^2} = \frac{2W_{\text{s}}(W_{\text{l}} - W_{\text{m}})}{W_{\text{l}}^2 + W_{\text{m}}^2 - 2W_{\text{l}}W_{\text{m}} - W_{\text{s}}^2}$$

$$\approx \tan[\theta_{\text{ccw}}(f) + \theta_{\text{cw}}(f)] \qquad (17)$$

For the L- versus M-cone plane, $\psi_{\text{l}} = 0$, $\psi_{\text{m}} = \pi/2$, $W_{\text{s}} = 0$, therefore

$$\tan[\theta_{\text{ccw}}(f)] = \frac{W_{\text{l}} \sin[\theta_{\text{l}}(f)] + W_{\text{m}} \cos[\theta_{\text{m}}(f)]}{W_{\text{l}} \cos[\theta_{\text{l}}(f)] - W_{\text{m}} \sin[\theta_{\text{m}}(f)]} \qquad (18)$$

$$\tan[\theta_{\text{cw}}(f)] = \frac{-W_{\text{l}} \sin[\theta_{\text{l}}(f)] + W_{\text{m}} \cos[\theta_{\text{m}}(f)]}{W_{\text{l}} \cos[\theta_{\text{l}}(f)] + W_{\text{m}} \sin[\theta_{\text{m}}(f)]} \qquad (19)$$

Projection of a cell's preferred vector in this plane is determined by its cone weights

$$\tan(\theta_{\text{Pref(LM)}}) = \frac{W_{\text{m}}}{W_{\text{l}}} \qquad (20)$$

If the response phases to L-, and M-cones are similar $\theta_{\text{l}}(f) \approx \theta_{\text{m}}(f)$, the preferred vector can be estimated by the average of CCW and CW response phases

$$\tan(2\theta_{\text{Pref(LM)}}) = \frac{2\dfrac{W_{\text{m}}}{W_{\text{l}}}}{1 - \left(\dfrac{W_{\text{m}}}{W_{\text{l}}}\right)^2} = \frac{2W_{\text{l}}W_{\text{m}}}{W_{\text{l}}^2 - W_{\text{m}}^2} \approx \tan[\theta_{\text{ccw}}(f) + \theta_{\text{cw}}(f)] \qquad (21)$$

For the L+M versus S-cone plane, $\psi_{\text{l}} = \psi_{\text{m}} = \pi/2$, $\psi_{\text{s}} = 0$, therefore

$$\tan[\theta_{\text{ccw}}(f)] = \frac{W_{\text{l}} \cos[\theta_{\text{l}}(f)] + W_{\text{m}} \cos[\theta_{\text{m}}(f)] + W_{\text{s}} \sin[\theta_{\text{s}}(f)]}{-W_{\text{l}} \sin[\theta_{\text{l}}(f)] - W_{\text{m}} \sin[\theta_{\text{m}}(f)] + W_{\text{s}} \cos[\theta_{\text{s}}(f)]} \qquad (22)$$

$$\tan[\theta_{\text{cw}}(f)] = \frac{W_{\text{l}} \cos[\theta_{\text{l}}(f)] + W_{\text{m}} \cos[\theta_{\text{m}}(f)] - W_{\text{s}} \sin[\theta_{\text{s}}(f)]}{W_{\text{l}} \sin[\theta_{\text{l}}(f)] + W_{\text{m}} \sin[\theta_{\text{m}}(f)] + W_{\text{s}} \cos[\theta_{\text{s}}(f)]} \qquad (23)$$

Projection of a cell's preferred vector in this plane is determined by its cone weights

$$\tan(\theta_{\text{Pref(LumS)}}) = \frac{W_{\text{l}} + W_{\text{m}}}{W_{\text{s}}} \qquad (24)$$

If the response phases to L-, M-, and S-cones are similar $\theta_{\text{l}}(f) \approx \theta_{\text{m}}(f) \approx \theta_{\text{s}}(f)$, the preferred vector can be estimated by the average of CCW and CW response phases

$$\tan(2\theta_{\text{Pref(LumS)}}) = \frac{2\dfrac{W_{\text{l}} + W_{\text{m}}}{W_{\text{s}}}}{1 - \left(\dfrac{W_{\text{l}} + W_{\text{m}}}{W_{\text{s}}}\right)^2} = \frac{2W_{\text{s}}(W_{\text{l}} + W_{\text{m}})}{W_{\text{s}}^2 - W_{\text{l}}^2 - W_{\text{m}}^2 - 2W_{\text{l}}W_{\text{m}}}$$

$$\approx \tan[\theta_{\text{ccw}}(f) + \theta_{\text{cw}}(f)] \qquad (25)$$

REFERENCES

Baylor DA, Nunn BJ, and Schnapf JL. Spectral sensitivity of cones of the monkey *Macaca fascicularis. J Physiol* (*Lond*) 390: 145–160, 1987.

Boycott BB and Wässle H. Morphological classification of bipolar cells of the primate retina. *Eur J Neurosci* 3: 1069–1088, 1991.

Boynton RM and Kambe N. Chromatic difference steps of moderate size measured along theoretically critical axes. *Color Res Appl* 5: 13–23, 1980.

Buchsbaum G and Gottschalk A. Trichromacy, opponent colours coding and optimum colour information transmission in the retina. *Proc R Soc Lond B Biol Sci* 220: 89–113, 1983.

Cavanagh P, MacLeod D, and Anstis S. Equiluminance: spatial and temporal factors and the contribution of blue-sensitive cones. *J Opt Soc Am A* 4: 1428–1438, 1987.

Chatterjee S and Callaway EM. S cone contributions to the magnocellular visual pathway in macaque monkey. *Neuron* 35: 1135–1146, 2002.

Dacey DM, Lee BB, Stafford DK, Pokorny J, and Smith VC. Horizontal cells of the primate retina: cone specificity without spectral opponency. *Science* 271: 656–659, 1996.

Derrington AM, Krauskopf J, and Lennie P. Chromatic mechanisms in lateral geniculate nucleus of macaque. *J Physiol* 357: 241–265, 1984.

DeValois R, Abramov I, and Jacobs GH. Analysis of response patterns of LGN cells. *J Opt Soc Am A* 56: 966–977, 1966.

Eisner A and MacLeod D. Blue sensitive cones do not contribute to luminance. *J Opt Soc Am A* 70: 121–123, 1980.

Eisner A and MacLeod D. Flicker photometric study of chromatic adaptation: selective suppression of cone inputs by colored backgrounds. *J Opt Soc Am A* 71: 705–718, 1981.

Gegenfurtner KR, Kiper DC, Beusmans JM, Carandini M, Zaidi Q, and Movshon JA. Chromatic properties of neurons in macaque MT. *Vis Neurosci* 11: 455–466, 1994.

Johnson EN, Hawken MJ, and Shapley R. The spatial transformation of color in the primary visual cortex of the macaque monkey. *Nat Neurosci* 4: 409–416, 2001.

Johnson EN, Hawken MJ, and Shapley R. Cone inputs in macaque primary visual cortex. *J Neurophysiol* 91: 2501–2514, 2004.

Kaiser PK, Lee BB, Martin PR, and Valberg A. The physiological basis of the minimally distinct border demonstrated in the ganglion cells of the macaque retina. *J Physiol* 422: 153–183, 1990.

Lankheet MJ, Lennie P, and Krauskopf J. Temporal-chromatic interactions in LGN P-cells. *Vis Neurosci* 15: 47–54, 1998.

Lee BB, Dacey DM, Smith VC, and Pokorny J. Horizontal cells reveal cone type-specific adaptation in primate retina. *Proc Natl Acad Sci USA* 96: 14611–14616, 1999.

Lee BB, Kremers J, and Yeh T. Receptive fields of primate retinal ganglion cells studied with a novel technique. *Vis Neurosci* 15: 161–175, 1998.

Lee BB, Martin PR, and Valberg A. The physiological basis of heterochromatic flicker photometry demonstrated in the ganglion cells of the macaque retina. *J Physiol* 404: 323–347, 1988.

Lee BB, Martin PR, and Valberg A. Nonlinear summation of M- and L-cone inputs to phasic retinal ganglion cells of the macaque. *J Neurosci* 9: 1433–1442, 1989.

Lee BB, Martin PR, Valberg A, and Kremers J. Physiological mechanisms underlying psychophysical sensitivity to combined luminance and chromatic modulation. *J Opt Soc Am A* 10: 1403–1412, 1993.

Lee BB, Pokorny J, Smith VC, and Kremers J. Responses to pulses and sinusoids in macaque ganglion cells. *Vision Res* 34: 3081–3096, 1994.

Lee BB, Pokorny J, Smith VC, Martin PR, and Valberg A. Luminance and chromatic modulation sensitivity of macaque ganglion cells and human observers. *J Opt Soc Am A* 7: 2223–2236, 1990.

Lee BB and Sun H. Chromatic input to cells of the magnocellular pathway: mean chromaticity and the relative phase of modulated lights. *Vis Neurosci* 21: 309–314, 2004.

Lee BB, Valberg A, Tigwell DA, and Tryti J. An account of responses of spectrally opponent neurons in macaque lateral geniculate nucleus to successive contrast. *Proc R Soc Lond B Biol Sci* 230: 293–314, 1987.

Lee SC, Jusuf PR, and Grünert U. S-cone connections of the diffuse bipolar cell type DB6 in macaque monkey retina. *J Comp Neurol* 474: 353–363, 2004.

Lennie P, Haake PW, and Williams DR. The design of chromatically opponent receptive fields. In: *Computational Models of Visual Processing*, edited by Landy M and Movshon J. Cambridge, MA: MIT Press, 1991, 337–348.

Lennie P, Krauskopf J, and Sclar G. Chromatic mechanisms in striate cortex of macaque. *J Neurosci* 10: 649–669, 1990.

Lennie P, Pokorny J, and Smith VC. Luminance. *J Opt Soc Am A* 12: 1283–1293, 1993.

Martin PR and Grünert U. Analysis of the short wavelength-sensitive ("blue") cone mosaic in the primate retina: comparison of New World and Old World monkeys. *J Comp Neurol* 406: 1–14, 1999.

Mullen KT and Kingdom FA. Losses in peripheral colour sensitivity predicted from "hit and miss" post-receptoral cone connections. *Vision Res* 36: 1995–2000, 1996.

Parraga CA, Troscianko T, and Tolhurst DJ. Spatiochromatic properties of natural images and human vision. *Curr Biol* 12: 483–487, 2002.

Pokorny J, Smithson H, and Quinlan J. Photostimulator allowing independent control of rods and the three cone types. *Vis Neurosci* 21: 263–267, 2004.

Reid RC and Shapley RM. Spatial structure of cone inputs to receptive fields in primate lateral geniculate nucleus. *Nature* 356: 716–718, 1992.

Reid RC and Shapley RM. Space and time maps of cone photoreceptor signals in macaque lateral geniculate nucleus. *J Neurosci* 22: 6158–6175, 2002.

Shapiro AG, Pokorny J, and Smith VC. Cone-rod receptor spaces, with illustrations that use CRT phosphor and light-emitting-diode spectra. *J Opt Soc Am A* 13: 2319–2328, 1996.

Smith VC, Lee BB, Pokorny J, Martin PR, and Valberg A. Responses of macaque ganglion cells to the relative phase of heterochromatically modulated lights. *J Physiol* 458: 191–221, 1992.

Smith VC and Pokorny J. Spectral sensitivity of color-blind observers and the human cone photopigments. *Vision Res* 12: 2059, 1972.

Smith VC and Pokorny J. Spectral sensitivity of the foveal cone photopigments between 400 and 500 nm. *Vision Res* 15: 161–171, 1975.

Snoddderly DM, Brown PK, Delori FC, and Auran JD. The macular pigment. I. Absorbance spectra, localization, and discrimination from other yellow pigments in primate retinas. *Invest Ophthalmol Vis Sci* 25: 660–673, 1984.

Stockman A, MacLeod DIA, and DePriest DD. The temporal properties of the human short-wave photoreceptors and their associated pathways. *Vision Res* 31: 189–208, 1991.

Stockman A, MacLeod D, and LeBrun SJ. Faster than the eye can see: blue cones respond to rapid flicker. *J Opt Soc Am A* 10: 1396–1402, 1993.

Stromeyer CFI, Eskew RT, Kronauer RE, and Spillmann L. Temporal phase response of the short-wave cone signal for color and luminance. *Vision Res* 31: 787–803, 1991.

Tansley B and Boynton R. A line, not a space, represents visual distinctness of borders formed by different colors. *Science* 191: 954–957, 1976.

Taylor AH and Kerr GP. The distribution of energy in the visible spectrum of daylight. The distribution of energy in the visible spectrum of daylight. *J Opt Soc Am A* 31: 3–8, 1941.

Valberg A and Tansley B. Tritanoptic purity-difference function to describe the properties of minimally distinct borders. *J Opt Soc Am A* 67: 1330–1336, 1977.

Vos JJ and Walraven PL. On the derivation of the foveal receptor primaries. *Vision Res* 11: 799–818, 1971.

Westheimer G. The Maxwellian view. *Vision Res* 6: 669–682, 1966.

Wiesel T and Hubel DH. Spatial and chromatic interactions in the lateral geniculate body of the rhesus monkey. *J Neurophysiol* 29: 1115–1156, 1966.

Yeh T, Lee BB, and Kremers J. The temporal response of ganglion cells of the macaque retina to cone-specific modulation. *J Opt Soc Am A* 12: 456–464, 1995.

Zaidi Q. Decorrelation of L- and M-cone signals. *J Opt Soc Am A* 14: 3430–3431, 1997.

Zaidi Q and Halevy D. Chromatic mechanisms beyond linear opponency. In: *From Pigments to Perception*, edited by Valberg A and Lee BB. London: Plenum Press, 1991, p. 71–82.

Zaidi Q and Halevy D. Visual mechanisms that signal the direction of color changes. *Vision Res* 33: 1037–1051, 1993.

Volume 95, February 2006

Sun H, Smithson HE, Zaidi Q, Lee BB. Specificity of Cone Inputs to Macaque Retinal Ganglion
Cells. *J Neurophysiol* 95: 837–849, 2006; doi:10.1152/jn.00714.2005; http://jn.physiology.org/cgi/
content/full/95/2/837.

Figure 1 contains errors in the numerical data in plots on the lefthand side. For *plot A1*: +S (0.67,
0.33, 0.35) should be changed to −S (0.67, 0.33, 0.35), +L−M (0.58, 0.42 1.0) should be changed
to −L+M (0.58, 0.42 1.0); for *plot B1*: −L+M (0.53, 0.26, 1.0) should be changed to −L−M
(0.53, 0.26, 1.0); *plot C1*: +S (0.67, 0.33, 1.0) should be changed to +S (0.67, 0.33, 1.65), +S
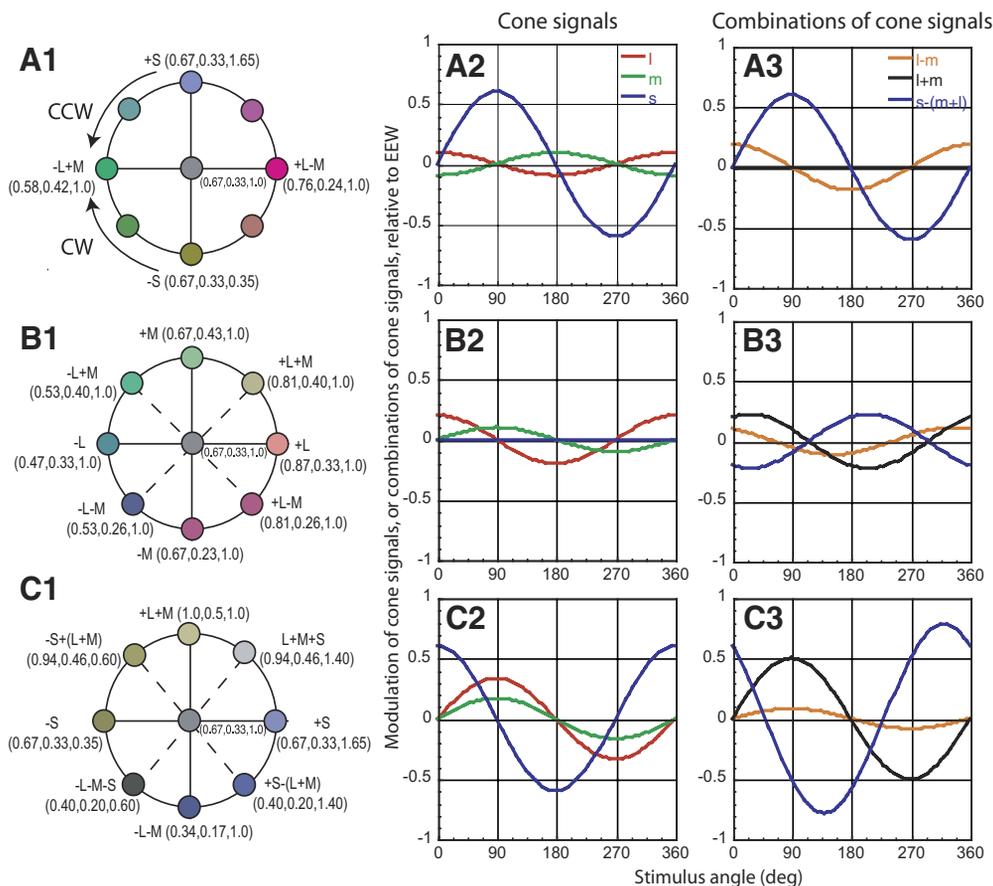(0.67, 0.33, 0.35) should be changed to −S (0.67, 0.33, 0.35). A corrected version of Fig. 1 appears
here.

FIG. 1. Chromaticity of a uniform field was modulated around a color circle in clockwise (CW) or counterclockwise (CCW) directions in an equiluminant
plane (*A1*), an long (L)- vs. medium (M)-cone plane (*B1*), or an L+M vs. short (S)-cone plane (*C1*). Numbers in *A1–C1* indicate Boynton-Kambe chromaticity
coordinates (L, M, S) for each point, and colored circles approximate stimulus appearance. Variation of L-, M-, and S-cone signals for the 3 planes are shown
in *A2–C2,* and combinations of cone signals L-M, L+M, and S-(L+M) are shown in *A3–C3,* respectively. *C1–C3*: 50% L+M contrast condition.